A spatially explicit study of prey–predator interactions in larval fish: assessing the influence of food and predator abundance on larval growth and survival

P. PEPIN,[1,*] J. F. DOWER[2] AND F. J. M. DAVIDSON[3]

[1]*Fisheries and Oceans, P.O. Box 5667, St John's, Newfoundland, Canada A1C 5X1*
[2]*Department of Biology and School of Earth and Oceans Sciences, University of Victoria, P.O. Box 3020, Victoria, British Columbia, Canada V8W 3N5*
[3]*Department of Physics and Physical Oceanography, Memorial University of Newfoundland, St John's, Newfoundland, Canada A1B 3X7*

ABSTRACT

We apply a coupled biophysical model to reconstruct the environmental history of larval radiated shanny in Conception Bay, Newfoundland. Data on the larvae, their prey and predators were collected during a 2-week period. Our goal was to determine whether environmentally explicit information could be used to infer the characteristics of individual larvae that are most likely to survive. Backward drift reconstruction was used to assess the influence of variations in the feeding environment on changes in the growth rates of individual larvae. Forward drift projections were used to assess the impact of predators on mortality rates as well as the cumulative density distribution of growth rates in the population of larvae in different areas of the bay. There was relatively little influence of current feeding conditions on increment widths. Patterns of selective mortality indicate that fast-growing individuals suffered higher mortality rates, suggesting they were growing into a predator's prey field. However, the mortality rates appeared to increase with decreasing predator abundance, based on the drift reconstructions. The relationship of growth and mortality with environmental conditions suggests that short-term, small-scale variations in environmental history may be difficult to describe accurately in this relatively small system (~1000 km^2).

*Correspondence. e-mail: pepinp@dfo-mpo.gc.ca
Received 1 March 2001
Revised version accepted 22 April 2002

Key words: capelin, drift modelling, feeding, fish larvae, predation, radiated shanny

INTRODUCTION

Which individual fish larvae survive from hatch to metamorphosis (or some other ecological or physiological shift) depends not only on each individual's growth rate but also on the spatial and temporal pattern in the selective forces (e.g. size selective feeding or mortality). Regional differences in feeding and growth may alter the relative susceptibility to impact by predators (Rilling and Houde, 1999) and the variable movement of highly active and migratory predators, such as pelagic fish, may result in differential survival. For example, Paradis *et al.* (1999) found that variations in the timing of simulated predation pressure resulted in substantial difference in the growth rates of surviving fish larvae.

How we investigate the effect of environmental conditions on either individual growth histories or their distribution is critical. To determine how an individual responds to changes in its feeding environment requires that we be able to reconstruct the advective history of that individual, at least in a general sense. Furthermore, we must consider that the growth of an individual at some age x is likely to depend on the growth rate of that individual during previous days (Mosegaard *et al.*, 1988; Pepin *et al.*, 2001). If, on the other hand, we are concerned with the selective removal of individuals from a population (e.g. by predators), then we cannot focus on individual growth rates but rather on the distribution of growth rates within the population. We must then project the pattern of drift forward for different parcels of the population to predict the changes in the distribution of growth histories, or any other measure of condition (Pepin *et al.*, 1999), in relation to the environmental conditions that they encounter. The key point is that larval health cannot be inferred from *in situ* environmental conditions at the time of sampling. A larva's condition will depend on environmental conditions faced prior and pursuant to time of sampling, during

which transport by surrounding currents can be important. We must also be able to predict where they came from (or are going to) and what conditions they have encountered (or will encounter) along the way.

Patch studies have been used to track the movement of larval fish but they provide a detailed view of only a small portion of the population, and they can generally be carried out for only short periods of time (Davis *et al.*, 1991; Murdoch and Quigley, 1994; Pepin *et al.*, 2002). An alternative is to couple survey observations with a dynamic circulation model that provides a reliable forecast of the variations in current speed and direction over the study area (Bowen *et al.*, 1995; Taggart *et al.*, 1996). Patterns of transport and dispersal can then be used to develop both the recent history and the future trajectories of individuals caught at each sampling site either by backward or forward projections of the model. The approach will be limited by the accuracy of the circulation model and the temporal horizon of the projections.

In this study, we apply this approach to study patterns of growth and survival of radiated shanny larvae (*Ulvaria subbifurcata*). Our observations are based on three surveys of Conception Bay (47°45′N, 53°00′W) during which we sampled both the ichthyoplankton and their prey. In addition, we also monitored the abundance of capelin (*Mallotus villosus*), the dominant planktivorous pelagic fish in the area, using hydroacoustic surveys. Larval growth histories were derived from measurements of otolith microstructure, while larval drift trajectories were simulated using a fine-resolution, wind-driven, three-dimensional (3-D) eddy resolving ocean circulation model. Our study of the effect of environmental conditions on the growth rate of individual larvae will be based on backward projections of drift while the effect of predator-induced mortality, and selective removal from the population, will be based on forward drift projections.

MATERIALS AND METHODS

Field sampling

Larval radiated shanny (also referred to as *Ulvaria* hereafter) were collected in Conception Bay, Canada (47°45′N, 53°00′W). Details of the study site were described previously by Laprise and Pepin (1995). Three surveys, each separated by 1 week, were conducted between 20 July and 5 August 1998. Ichthyoplankton were sampled at 19–23 stations spaced approximately 8 km apart (Fig. 1). Each survey was completed in approximately 24 h. At each station, a single oblique tow (0–40 m) was performed using a 4 m^2 Tucker trawl equipped with sections of 1000-, 570-, and 333-μm-mesh Nitex (Pepin and Shears, 1997) and towed for 10–15 min at 1 m s^{-1}. This gear is an effective sampler of larval fish up to 20–25 mm and the large sample volume results in high precision (Pepin and Shears, 1997). Volume filtered was estimated as the average of two General Oceanics flowmeters located at the mouth of the net. Samples were preserved in 95% ethanol for one week, following which samples were drained to replace the preservative. Ichthyoplankton were sorted and identified to species or to the lowest taxonomic level possible. Length frequency distributions for each species and sample were estimated by measuring up to 200 larvae. Standard lengths were measured to the nearest millimetre using a dissecting microscope and a grided background.

Microzooplankton were sampled using a 0.5-m-diameter plankton net (70-μm mesh) hauled vertically from 40 m to the surface (1 m s^{-1}). The sample was preserved in 2% buffered formaldehyde. The abundance of copepod nauplii was estimated by sequential fractionation of the sample using a Matoda splitter

Figure 1. Map of survey area and station locations. The solid line represents the separation between the inner and outer portions of the bay. Bell Island is the land mass located on the eastern side of the bay. Closed circles indicate stations that were used in the tracking of particles in drift projections; open triangles were not used in the tracking of particles but were sampled during each survey. The location of St John's airport is shown by the grey circle.

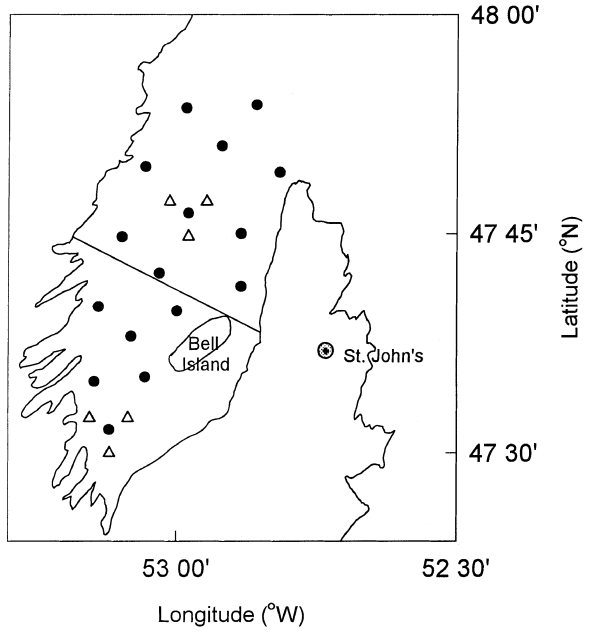

until approximately 200 individuals could be enumerated.

Temperature, salinity and fluorescence profiles of the water column were obtained at each station using a Seabird-25 CTD (sampling rate of 8 Hz) lowered at a rate of 1 m s^{-1} to within 5 m of the bottom.

Currents were measured using a hull-mounted RDI 153-kHz acoustic Doppler current profiler (ADCP) in bottom-track mode to provide a basis for comparison with the circulation model. Data from the ADCP were recorded in 4-m depth bins (first bin at 7–11 m). A sampling interval of 3 min was used to give a nominal ensemble average based on at least 50 pings. The standard deviation of unsmoothed single-bin currents was ~0.03–0.05 m s^{-1}.

Abundance of juvenile and adult capelin was estimated using a calibrated hull-mounted split-beam 38-kHz transducer and an EK500 echosounder system. Backscatter volume (S_v) measurements were acquired at a threshold of −75 dB in depth bins of 520, 20–35, 35–50, 50–75, 75–100 and 100–200 m. Capelin were distinguished from other fish backscatter using echogram characteristics combined with species composition and biological characteristics obtained during fishing sets. Biological data originated from 21 tows using an IYGPT trawl at a number of sites in Conception Bay conducted during the course of the study. Backscatter (S_v) values originating from capelin were integrated over the whole water column (5–200 m) in 3-min intervals to produce estimates of the backscatter area (S_a) in m^2/m^2 (MacLennan and Simmonds, 1992). Backscatter values originating from the top 5 m were generally not included because capelin above or near the transducer is not detected by the acoustic method. S_a was then scaled to numbers of individuals per square meter by applying the length–frequency distribution of capelin, sampled during IYGPT trawls, and the target strength relationship $20 \log L - 73.1$, where L is length in centimetres (Rose, 1998).

Otolith microstructure analysis

Body measurements of larval shanny were taken using an Optimas® image analysis system (V.4.1) connected to a dissecting microscope. An Olympus BH-2 compound microscope (500× magnification) and the imaging system were used for all otolith measurements. Prior to otolith extraction, each animal was assigned a unique identifier number and measured for standard and total length (to the nearest 0.1 mm). Lapillar and sagittal otoliths were extracted from 509 *Ulvaria* larvae (up to 10 larvae were selected at random from each station). Each otolith was mounted in a small drop of Crystal Bond® thermoplastic cement placed on a microscope slide. All subsequent analyses were performed using the sagitta, choosing the right or left otolith at random unless one proved impossible to read. Each otolith was ground to the midplane using 0.3-μm lapping film. Minimum and maximum radii as well as the hatch check were measured (in μm) relative to the nucleus of the otolith. Total area (μm^2) was estimated after identifying the periphery of the otolith. The operator then measured the width of each increment by marking the outer edge of that increment along the longest axis of each otolith, which occasionally required refocusing of the image. Throughout the analysis, we consider that each otolith increment represents 1 day. Analyses of patterns in increment widths were performed using data standardized to zero mean and unit standard deviation [$z_{i,j} = (x_{i,j} - \bar{x}_j)/s_j$, for specimen i in age interval j] because of the covariance between mean increment width and increasing age (Pepin *et al.*, 2001). Standardization of increment widths was carried out to simplify the description of patterns in growth rates for the reader, thus removing the age-dependent trends in the mean and variance in increment widths. The results, statistical analyses and conclusions are unchanged. Increment widths in radiated shanny provide a measure of the instantaneous growth in weight (Pepin *et al.*, 2001).

To assess the potential impact of selective mortality on the *Ulvaria* larvae, we had to contrast the distribution of growth histories from one survey to the next among larvae of the same age during the initial survey (e.g. we contrasted the otolith widths from 10-day-old larvae caught in the first survey with the widths found at age 10 in 17-day-old fish caught in the second survey). To achieve this, age-dependent cumulative probability distribution functions (CDF) were derived using local non-parametric density estimation (Pepin *et al.*, 1999). The CDF of increment widths from one survey was then contrasted with the CDF for larvae caught in the subsequent survey at the ages they had during the earlier survey. Because of the degree of autocorrelation in adjacent increment widths (Pepin *et al.*, 2001), the data from each individual also included widths from the three increments preceding the day of capture (for the initial conditions) or the back-calculated age during the initial survey (for the larvae captured in surveys 2 or 3). The significance of changes in the age-dependent pattern of median standardized increment width of the population was determined by calculating the 95% confidence intervals of the median using randomization.

Drift simulations

Simulations of the circulation during the study period were performed with an application of the 3-D eddy-resolving CANDIE model to Trinity and Conception Bay (Davidson *et al.*, 2001). This *z*-coordinate model solves the 3-D nonlinear Navier–Stokes equations on an *f*-plane using the hydrostatic, Boussinesq and rigid-lid approximations. The equations are finite-differenced on a 3-D, Arakawa C-grid with 1 km horizontal and 10 m vertical resolution. The model resolution easily resolves the first baroclinic Rossby radius that is approximately 5 km. A free-slip condition is applied on the lateral land boundaries. The model domain comprised a realistic bottom topography of Conception Bay, and of adjacent Trinity Bay to the north, whose wind-driven circulation influences that of Conception Bay by coastal-trapped wave propagation (Davidson *et al.*, 2001). The open boundary conditions are similar to those of Greatbatch and Otterson (1991) and designed to prevent spurious upwelling at the juncture of land and the model's open boundaries.

All circulation model runs are initialized at rest (i.e. no motion) with horizontally uniform stratification based on the long-term mean (1957–97) for the month of July at Station 27 (approximately 20 km south of the mouth of Conception Bay). The model is run with spatially uniform wind stress based on observations at St John's Airport, situated 10 km east of Conception Bay. Wind stress is introduced over 2 days using a hyperbolic tangent ramping function starting on day 190 and running for 35 days. Particles are released on day 201 at 12.00 hours. The drifter mode implemented is described in Davidson and deYoung (1995) and is designed to track particles smoothly through a finite-resolution velocity field. There is no vertical transport of drifters so particles are constrained to a 2-D velocity field within each layer. Particles will thus accumulate near the coast where downwelling occurs. The drifters were given a random walk component to their displacement at every time step equivalent to a diffusion coefficient of 10 $m^2\ s^{-1}$. This allows for particles seeded at the same location in the model to be dispersed from each other over time.

We analysed the patterns of drift for the top two modelled layers (0–10 and 10–20 m) that correspond to the observed vertical distribution of larvae in the upper water column. As the results were similar for both layers, despite differences in responsiveness to wind forcing, we only present the results from the deeper layer, for the sake of brevity. Backward projections of larval drift tracks were conducted by uniformly seeding the model domain with particles (0.5 km apart) on days 201 and 208 and simulating their drift for 7 days. After the 7-day drift period (ending on days 208 and 215, respectively), particles were consider to be associated with a station location if they were within 3 km of the sampling site. Forward projections were performed by seeding 1000 particles within a 1-km radius of the stations sampled on days 201 and 208 and forecasting their drift for a 7-day period. A 14-day forward simulation was also performed starting with the station locations sampled on day 201.

Because we cannot assign the behaviour of an individual particle to an individual larva caught at a sampling location, we calculated the average drift trajectory of the particles assigned to each station for both the backward or forward projections. Owing to dispersion of particles, this introduces increasing uncertainty of particle location with elapsed time (forward or backward) from sampling point and leads to greater uncertainty about the environmental conditions encountered by larvae.

Environmental reconstructions were based on the observations collected during each of the three surveys. For each realization, data from stations (for copepod nauplii) or continuous collections (for pelagic fish) were interpolated onto a 1-km grid. In the case of nauplii, changes in environmental conditions from one survey to the next were linearly interpolated through time at each grid point. The conditions encountered by the larvae from each station (either in backward or forward projections) were then determined using the positional information from the average drift trajectory at daily intervals from the start to the end of each simulation period. When the average drift trajectory wandered outside the area within which we could interpolate environmental conditions, we did not attempt to extrapolate conditions to the station's position. Environmental reconstructions were performed for each 7-day period between surveys.

Forward drift projections were used to investigate patterns of mortality. The concentration of larvae from each station sampled on day 201 or 208 was moved to the model's projected location and contrasted with the abundance of larvae observed on days 208 and 215, respectively. To account for the effects of growth, the abundance of larvae of length l (each interval being of 1 mm) on day t was contrasted with the abundance of larvae of length $l + 2$ observed on day $t + 7$ and mortality rates were calculated as $Z = \ln(N_{l+2,t+7}/N_{l,t})$, where N is the concentration of larvae. Note that mortality is represented by negative values of Z. Our choice of a 2-mm increment

is based on observed growth rates (see below). Note that a negative value of Z indicates population loss whereas a positive value indicates production or influx.

RESULTS

Environmental conditions

Winds were predominantly from the southwest at average speeds of 20 km h^{-1} and rarely exceeding 30 km h^{-1} (Fig. 2). There were two instances where the wind shifted to westerly/northerly direction and average speeds decreased to ~10 km h^{-1}. These bouts lasted 28 and 36 h and were generally preceded by periods with weak southwesterly winds. There was also a short period of weak westerly winds toward the end of the study period.

Surface temperature exhibited similar spatial patterns during all surveys, with warmer waters on the eastern side and cooler ones in the western region (Fig. 3). There was a clockwise movement of the surface isotherms between the first and second surveys followed by a counter-clockwise movement with increasing sea surface temperature contrast between the second and third sampling periods (Fig. 3), indicative of upwelling.

Total copepod nauplii abundance was lowest during the first survey and highest during the second, with a subsequent decrease during the third survey (Fig. 3). Variations in the spatial distribution of nauplii from one survey to the next mimicked the shifts in the distribution of sea surface temperature (Fig. 3). There was a significant expansion of a region of high nauplii concentration during the second survey followed by a gradual retraction of the area toward the western side of the bay during the third survey. The variations were likely because of changes in local production and loss, as nauplii concentrations were not associated with specific water masses (Fig. 4).

Results from the 21 IGYPT tows conducted at night (0–100 m) indicated that capelin (55–185 mm) were the dominant fish in the water column, representing >96% of the biomass and >98% of the numbers in any single tow. Hydroacoustic returns indicated a steady 10-fold decrease in the abundance of pelagic fish during the course of the study (Fig. 3). During the first survey, capelins were broadly distributed throughout the study area, with the highest concentrations

Figure 2. Time series of wind speed (top panel) and direction (bottom panel) starting 5 days before the survey period (days 201–215) from St John's International Airport weather station. Data are recorded at hourly intervals.

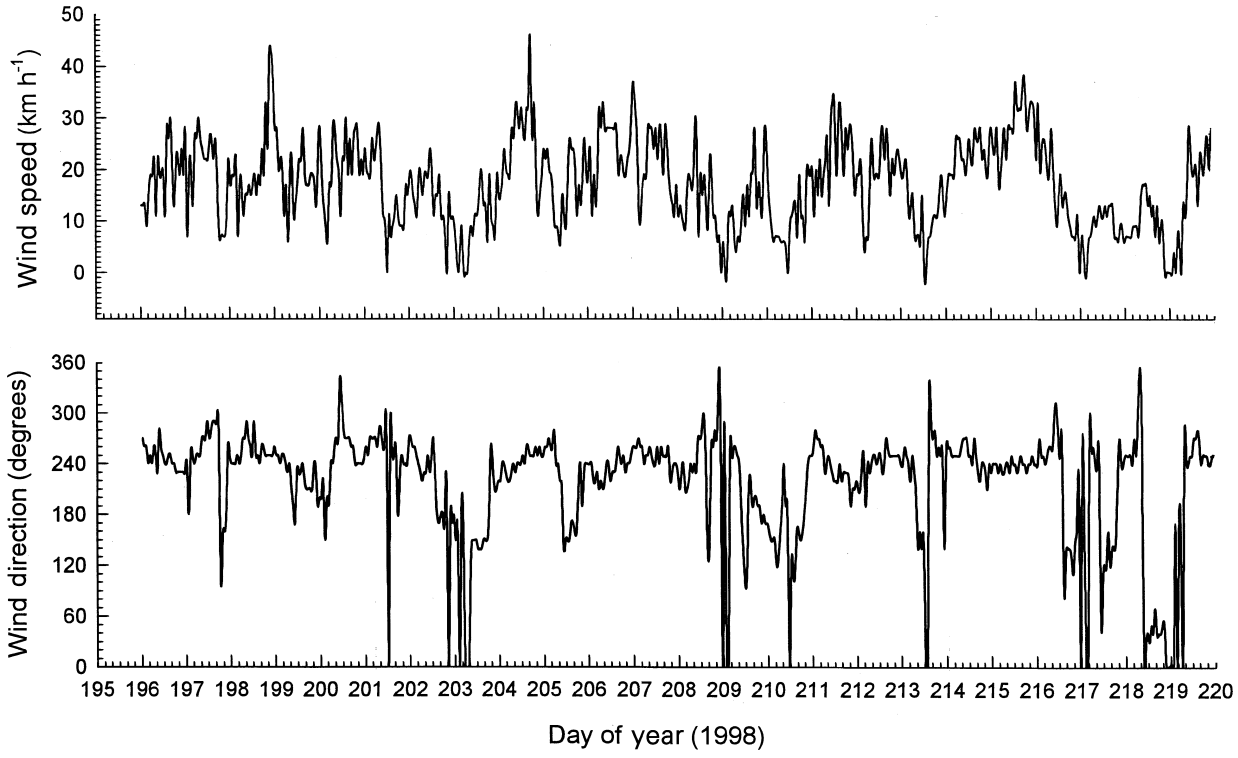

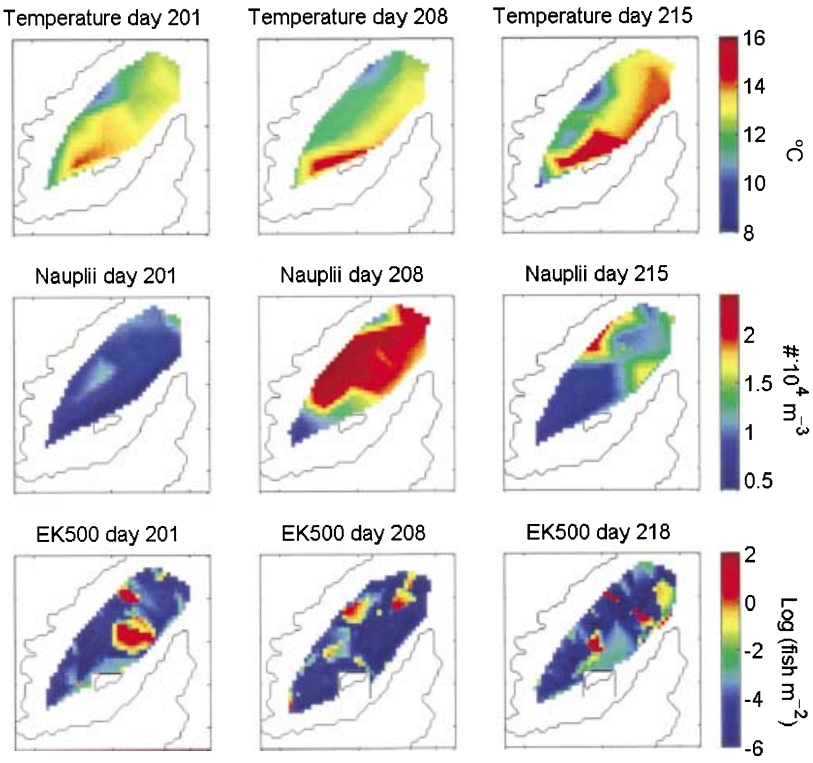

Figure 3. Temperature (°C; 5 m depth) field, average nauplii concentration ($\# \times 10^4$ m^{-3}; 0–40 m) and capelin density (fish m^{-2}; 5–200 m) based on linear interpolation of observations obtained during the three successive surveys of Conception Bay. The scale bar for each row is located next to the rightmost panel. Maps are plotted on idealized model coordinates with a 1-km grid.

occurring seaward of Bell Island (Fig. 3). The distribution of pelagic fish was somewhat patchier during the second sampling period, with the highest concentrations located on the western side of the bay but with most of the biomass still being found in the outer portion of the bay (Fig. 3). Low concentrations of pelagic fish were present throughout the bay during the third survey, with small areas of high concentrations scattered in the outer part of the bay (Fig. 3).

Figure 4. Bubble plot of nauplii density (# m^{-3}; 0–40 m average) in relation to temperature and salinity (5 m) from each sampling location.

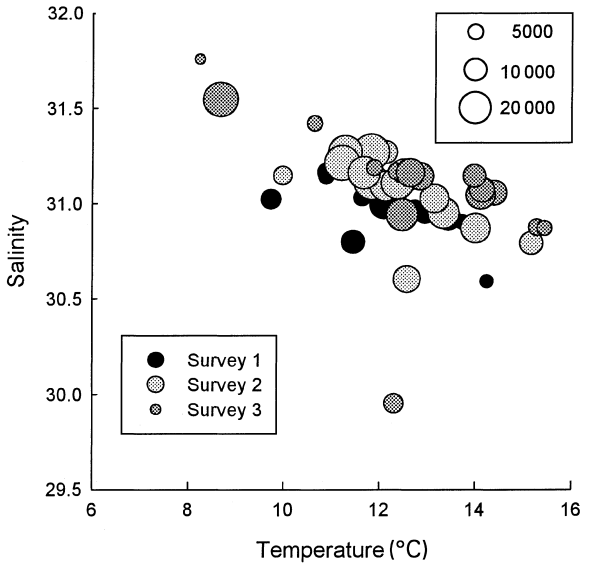

Vertically averaged currents, measured between 7 and 27 m using the ADCP, show considerable horizontal variability. There was evidence of counterclockwise recirculation in the outer portion of the bay during the first and third surveys and there was an area of divergence along the northeastern shore apparent during all three surveys. During the first survey, flow in the southern part of the bay was in a southerly direction on the eastern side and northwesterly on the western side. Currents measured during the second survey are directed into the bay along the western side and generally flow toward the mouth along the eastern shore. There was no discernable pattern observed during the third survey, other than a tendency for weak westerly or northerly currents along the western side. Currents became progressively weaker during the study period with an average of 8.7 cm s^{-1} (range: 1–29), 7.7 cm s^{-1} (range: 1–19) and 4.9 cm s^{-1} (range: 1–12) from the first to the third survey.

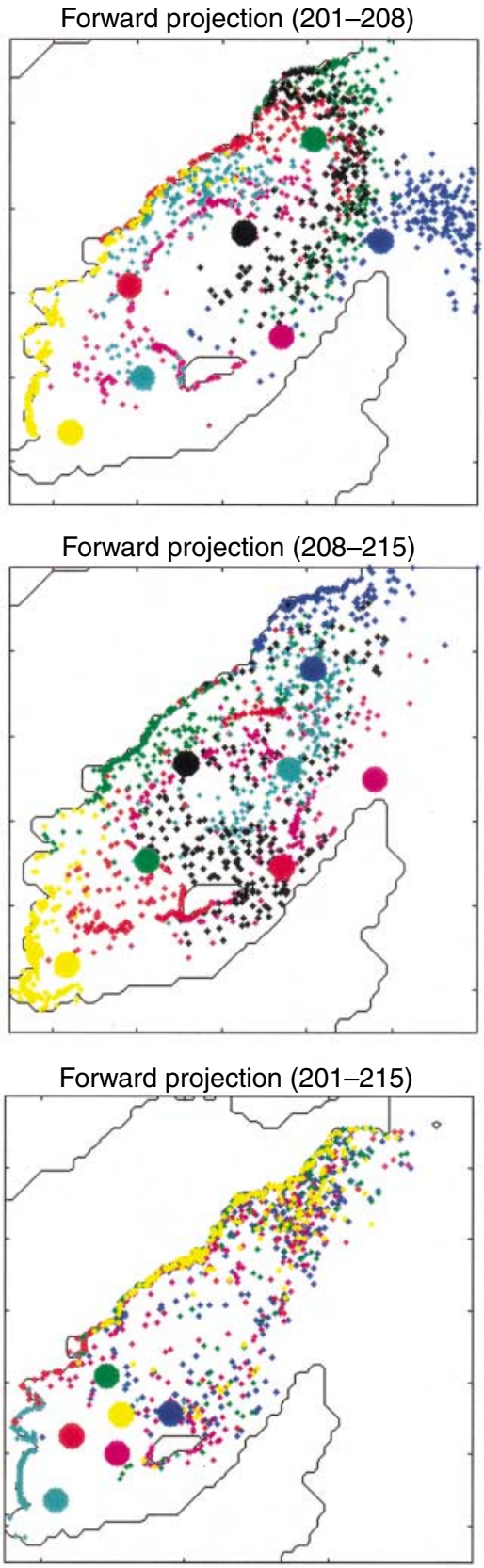

◄

Figure 5. Plot of forward drift projections for particles during the first (days 201–208) and second (days 208–215) week of the study period as well for the combined 2-week period (days 201–215). For each simulation, the initial position of particles in these plots started from the stations represented by the large coloured symbols and the final position of particles is represented by the smaller symbols of the same colour. Maps are plotted on idealized model coordinates with a 1-km grid.

Drift projections

The general modelled circulation pattern observed throughout the study period was characterized by a clockwise flow with a relatively strong north-eastward current along the western side (Fig. 5). Average drift trajectories suggest that movement of particles along the eastern side of the bay appears to have been somewhat less important during both projections but this is largely an artefact of the location of sampling sites that are used to initialize the simulations (Fig. 5). The trajectory of individual particles clearly shows the existence of a clockwise gyre with significant drift along the eastern side of the bay (Fig. 5). Currents, and thus drift, were stronger during the first part of the study (days 201–208) than during the second (days 208–215), in agreement with ADCP observations. There was also evidence of a retentive gyre in the outer portion of the bay during the latter period. Backward and forward projections indicate that the head of the bay is a major source of particles for the outer portion of the bay (Fig. 5). A 2-week projection of drift shows that most of the larvae that were at the head of the bay (based on six stations) at the start of the study (day 201) would have drifted into the outer portions of the study area by day 215 (Fig. 5).

Despite spatial differences in the distribution of prey and predators, the reconstructions of environmental histories were dominated by the major shifts in abundance that took place from one survey to the next (Fig. 6). The shift in mean nauplii concentration based on the backward projections from one survey to the next was substantially greater (~10 : 1) than the variability among stations within a survey (Table 1). Forward projections of predator condition showed that the shift in mean predator levels between surveys was slightly less than the variance among stations within surveys (Fig. 6).

The average growth rate of radiated shanny larvae, based on length at age of capture, was 0.29 mm day^{-1} ($F_{[1,504]} = 2830$, $P < 0.001$) and there were no statisti-

Figure 6. Reconstructed time series of projected nauplii and capelin densities (Nauplii: top row; Predators: bottom row) in relation to day of year for the first (left column) and second (right column) weeks of the study period. Drift projections were run for only 1 week to limit the effects of dispersal on the reconstructed history of larvae from each station location. Backward projections were run to determine the feeding history of individuals captured from each station and forward projections were run to describe the predator environment larvae would face. Each line represents the environmental history of particles from a single station. Broken or missing lines indicate the projected drift path moved particles outside the area over which we could interpolate the concentration of nauplii or capelin.

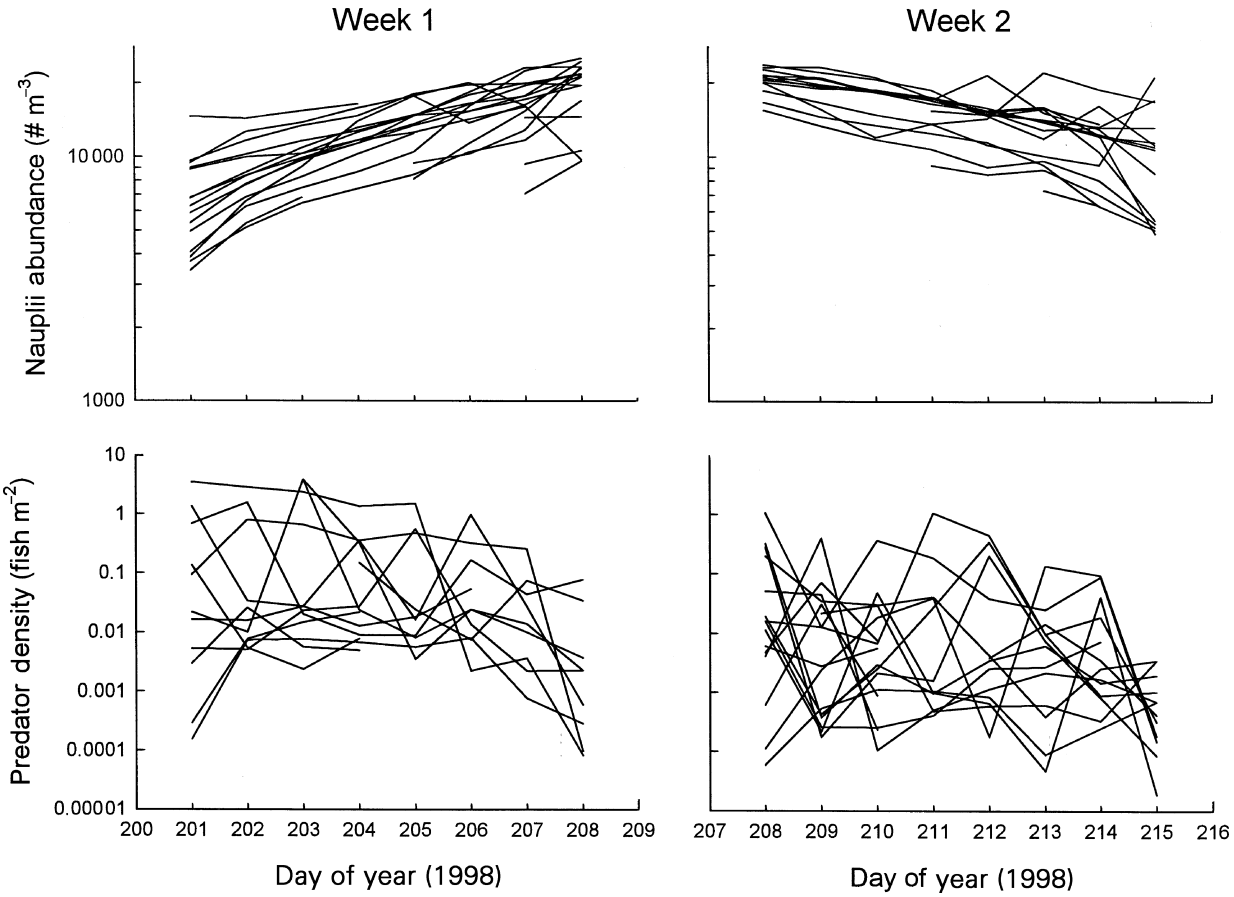

Table 1. Change in predicted (and interpolated) prey and predator concentrations from drift reconstructions (mean and variance in prey and predator abundance) for stations from which larvae (particles) were tracked between successive surveys. All data were log-transformed.

	Days 201–208	Days 208–215
Nauplii (# $\times 10^4$ m^{-3})		
$\bar{x}$ log(N)	3.80–4.24	4.31–3.98
S^2 log(N)	0.033–0.024	0.028–0.044
Predators (fish m^{-2})		
$\bar{x}$ log(P)	−0.81 to −1.85	−1.16 to −2.55
S^2 log(P)	1.61–1.18	0.45–1.41

cally significant differences among surveys ($F_{[2,504]} = 0.91$, $P > 0.5$) (Fig. 7). All analyses are based on *F*-values estimated using type III sum of squares.

Analysis of growth histories in relation to the reconstructed feeding environment from the backward drift projections was based on a linear model. The model we applied described the standardized increment width on day of life i (g_i) in relation to the average standardized increment width on the 3 days prior to day 201 or 208 (G), the forward lag from that day (Δt), and the concentration of nauplii encountered on day i (N_i) based on the backward drift simulations ($g_i = b_0 + b_1 g + b_2 \Delta t + b_3 N_i$, where *b*-values refer to regression coefficients). The older the larvae were, the stronger and more was direct the effect of their past history on their current growth, as indicated by the stronger and more direct (i.e. 1 : 1) relationship between current increment width and the individual's average growth rate (G) at the start of each survey period (Fig. 8). There was a negative

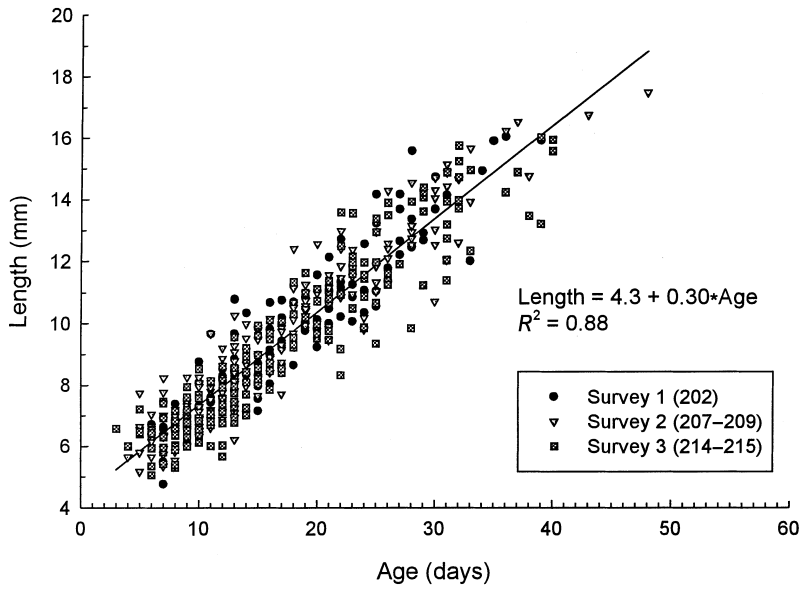

Figure 7. Length-at-age relationship for radiated shanny larvae captured during each of the three survey periods. Line represents least squares regression for all survey periods combined.

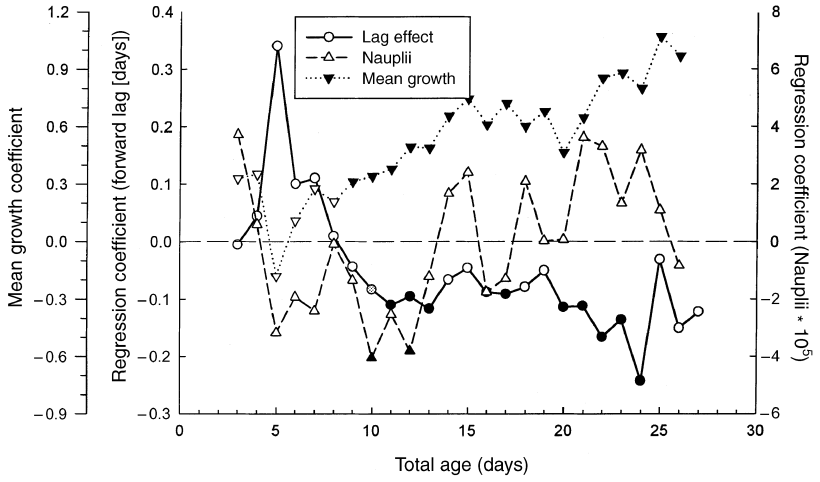

Figure 8. Regression coefficients of the relationship between current growth rates (total age of the larva on the day represented by each increment), the mean increment width at the start of the survey period (based on the three increments prior to day 201 or 208), the concentration of nauplii on the day of the growth increment, and the lag forward from day 201 or 208. Open symbols indicate a non-significant effect whereas closed symbols indicate $P < 0.05$.

effect on growth rate of the forward separation from the start of each simulation period, and this was significant for most ages between 10 and 25 days (Fig. 8). This effect is mostly an artefact of the standardization of increment widths coupled with the pattern of selective survival in relation to past growth (see below). Finally, there was little evidence of a significant effect of prey abundance on the growth of individual larvae (Fig. 8). Only for ages of 10 and 12 days post-hatch was the effect significant, and in those instances the relationship was negative. Regression coefficients for the prey abundances tended to be negative for ages 5–13 and mostly positive for ages 14–26. A runs test (Sokal and Rohlf, 1981, pp. 782–787) shows this pattern to be marginally significant ($P < 0.05$).

The overall pattern of changes in larval abundance clearly indicates that mortality rate increases with increasing length of larvae (Fig. 9). Note that mortality is represented by negative values of Z. The relationship between mortality rates and the history of predator encounters is in the opposite direction to expectations: there is a slight decrease in mortality rate with increases in the estimated predator field (Fig. 9). A multivariate general linear model revealed a strong significant effect of body length on mortality ($F_{III[1,139]} = 78.8$, $P < 0.001$) and a significant interaction of body length with predator density ($F_{III[1,139]} = 13.7$, $P < 0.05$). Restricting the analyses to 1-mm length intervals revealed that decreases in mortality rate with increasing predator density were only statistically significant in the largest size category

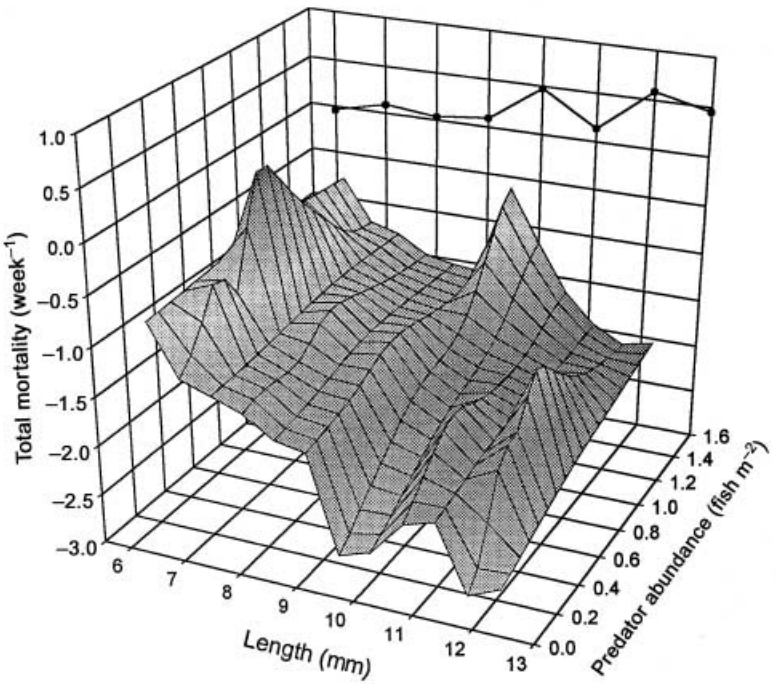

Figure 9. Three-dimensional, linearly interpolated surface of the total weekly mortality rate of larval radiated shanny in relation to their length at the start of the week and predator abundance estimated from the summed hydroacoustic integrated voltage. The line and symbol plot on the back panel shows the regression coefficient of the relationship between mortality rate and summed hydroacoustic integrated voltage for each 1-mm length interval.

(13 mm) but notable in all length intervals from 10 mm onwards (Fig. 9). In smaller length categories, the response to changes in reconstructed predator abundance was essentially flat. In some instances, there appears to have been an increase in abundance rather than a decrease, particularly in the smaller larvae during the first period of observation. This is partly because our approach to estimate the 'mortality history' does not allow for dispersal or aggregation of larvae in the model domain but, rather, uses the average drift path to determine the centre of mass of particles from each source station.

Because of the strong contrast in predator abundance between the inner and outer portions of the bay, we use the separation between stations above and below the northern tip of Bell Island to contrast the distribution of increment widths (based on the last three increments before capture) from one survey to the next. Larvae caught during the first survey in the inner bay showed an increasing median standardized increment width with increasing age in contrast to larvae in the outer bay, which showed a slight decrease (Fig. 10). The contrast in trends with age between regions is not quite as pronounced during the second survey but it is still present and increment widths in the inner bay are generally higher than in the outer bay (Fig. 10). There is almost no difference in the pattern of growth histories between the inner and outer bay during the final survey (Fig. 10).

To provide an appropriate contrast of the changes in the CDF of growth increments through time, we must take into consideration the results of the drift projection, which show substantial movement of larvae from the first survey from the inner to the outer portions of the bay (Fig. 5). In contrast, larvae from the outer bay tend to remain in that region, although there is some transport into the inner part of the study site. If we consider the inner bay exclusively, there is selective removal of faster growing larvae from the first through to the third survey (Fig. 11). Randomization tests show that the median increment width is significantly lower (i.e. the 95% confidence intervals overlap) during survey 2 for larvae that were ages 19 and beyond in survey 1 and for ages 9 and beyond when we contrast surveys 1 and 3. Perhaps a more appropriate comparison is to contrast larvae from the inner (survey 1) and outer bays (surveys 2 and 3), because the former would have essentially drifted into the outer reaches of Conception Bay based on our drift projections (Fig. 5). When we do so, the median increment width is significantly lower in larvae that would have been older than 10 and 4 days old during the first survey (Fig. 11) for the second and third surveys, respectively. The implication is that the cumulative effect of selective mortality was becoming more apparent in younger larvae from the first survey, but this also indicates that losses are greater in larger (older) individuals. When we contrast the distribution

Figure 10. Cumulative probability distribution function (CDF) of standardized increment widths, based on the 3 days prior to collection of each specimen, in relation to total age at capture. The three lines show the 10th, 50th and 90th percentiles of the CDF estimated using a local non-parametric density estimator with a bandwidth of 3 days. Inner and outer portions of the bay are identified in Fig. 1.

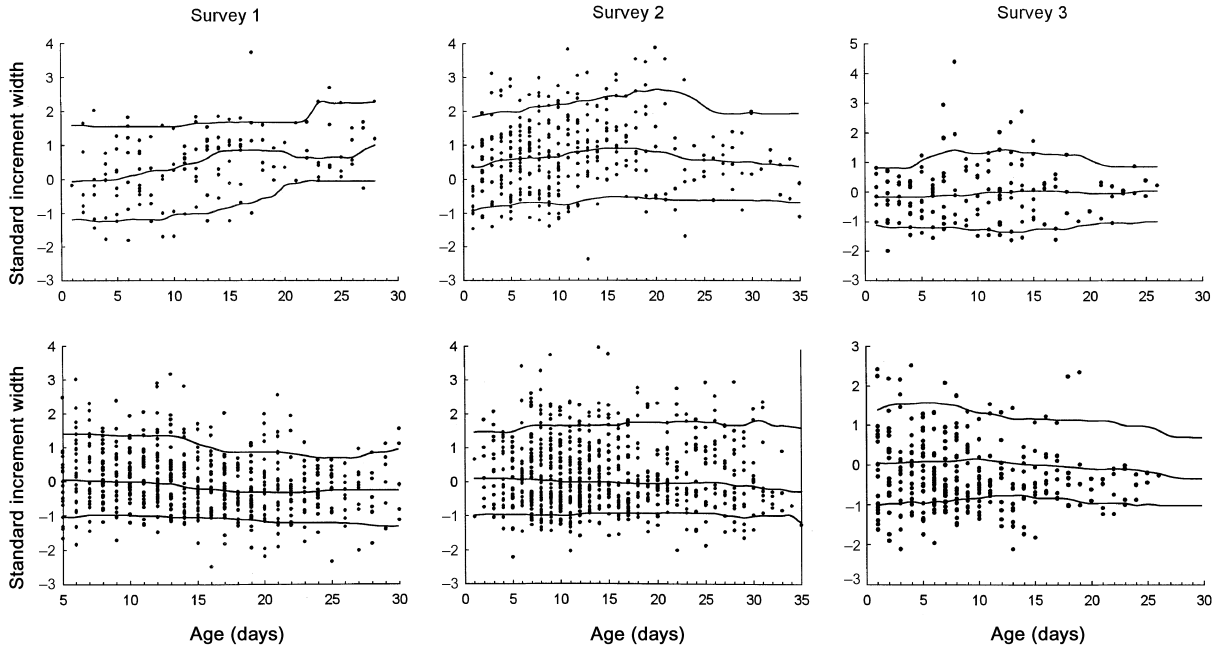

of standardized increment widths for larvae that would have remained exclusively in the outer bay, we find a significant decrease in median increment widths after 2 weeks (surveys 1 and 3) in larvae that were less than 15 days of age during the first survey but there is no significant difference in older larvae (Fig. 11). When we contrast larvae from the second and third surveys, we find significant differences in median increment width only between the inner and outer portions of the bay (Fig. 12). In virtually all instances, there is evidence of selective removal of faster-growing larvae during our study.

DISCUSSION

Growth histories of individuals and their distribution within the population have provided us with an indication about some of the processes acting on the dynamics of radiated shanny larvae. We were unable to find any compelling evidence that the environmental history significantly altered the growth of an individual, as others have observed (Gallego *et al.*, 1996). Individual growth rates were highly autocorrelated (this study; Pepin *et al.*, 2001). At the population level, there was clear evidence of selective mortality in which faster growing individuals were less likely to survive than individuals with lower growth rates. This is consistent with the pattern of increasing mortality with increasing body size, but inconsistent with the often cited 'bigger is better' hypothesis (Litvak and Leggett, 1992) emphasizing the importance of understanding prey–predator dynamics. However, we were again unable to find any significant relationship with projected environmental history (in this case predator abundance) consistent with fundamental expectations. One is left to question whether our projections of circulation were accurate and whether there was any benefit in developing environmental histories?

Conception Bay is a physically dynamic system that responds rapidly to variations in wind forcing as a result of both local and remote influences (deYoung *et al.*, 1993). Davidson *et al.* (2001) showed that their model was able to predict changes in surface circulation and isopycnal displacement. Prior to and during this study, winds were light and generally from a constant direction. Under southwesterly winds, upwelling prevails on the western side of the bay along with a broad coastal jet directed towards the mouth of the bay. Model projections indicated stronger currents during the first week of our study and weaker ones during the second. This is consistent with observed

Figure 11. Median and 95% confidence intervals of the median from cumulative probability distribution function (CDF) of growth rates in relation to age on day 201 (based on the three standardized increment widths prior to that day) for radiated shanny larvae (survey #1) from the inner and outer portions of Conception Bay. The larvae used to represent the CDF from each survey are based on the location of capture during each of the surveys. The inner and outer portions of the bay are defined in Fig. 1. The confidence intervals of the median were estimated from 500 randomizations of the data.

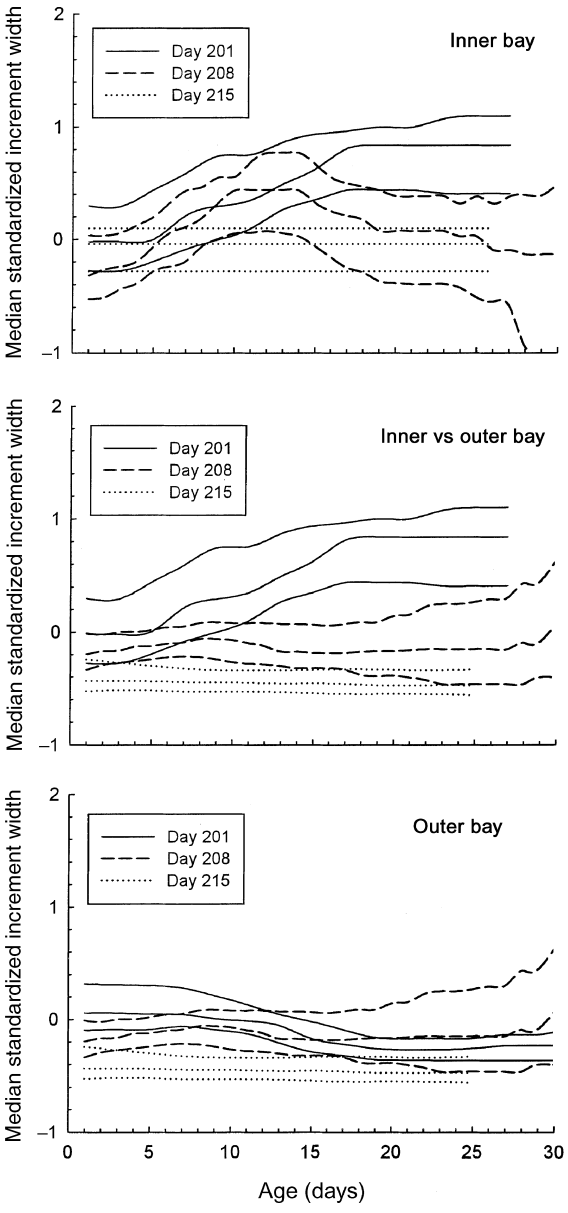

Figure 12. Median and 95% confidence intervals of the median from cumulative probability distribution function (CDF) of growth rates in relation to age on day 208 (based on the three standardized increment widths prior to that day) for radiated shanny larvae (survey #2) from the inner and outer portions of Conception Bay. The larvae used to represent the CDF from each survey are based on the location of capture during each of the surveys. The inner and outer portions of the bay are defined in Fig. 1. The confidence intervals of the median were estimated from 500 randomizations of the data.

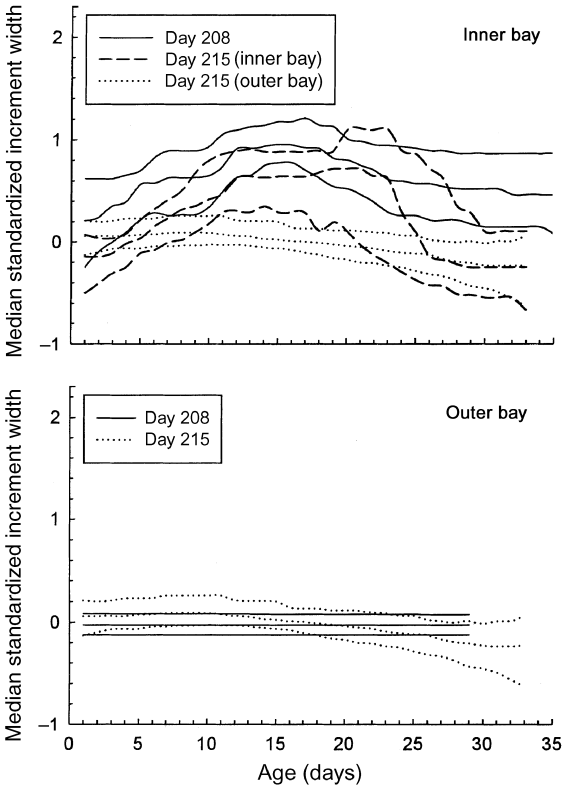

cold surface waters being more widely distributed during the second survey than in the first, and the subsequent retreat of cold surface waters by the third survey. Furthermore, temporal shifts in the spatial distribution of shanny larvae were consistent with the presence of a clockwise circulation field and an area of retention or convergence located in the northwestern quadrant of the system, as predicted by the circulation model. These observed patterns suggest that the general features of the circulation were adequately represented by model forecasts for the purposes of this study.

Environmental histories are essential if we are to understand the population dynamics of larval fish. We know from an analysis of measurement error of otolith microstructure that observations of environmental conditions at the time of capture are unlikely to yield much insight into the processes regulating growth

because the width of growth increments just before capture primarily reflect the effects of past rather than present events (Pepin *et al.*, 2001). However, without knowledge of the drift and the environment recently encountered by the larvae, we would not have been able to assess the possible influence of prey availability on increment width.

Spatial and temporal scales of the system under study and variations in the environmental conditions must also be considered. The general correspondence of changes in prey distribution with changes in the extent of cold water (and to a lesser extent the temporal variations in abundance) suggests that the general magnitude of fluctuations were reasonably well captured by our sampling programme. Fluctuations in nauplii abundance are likely to follow scales that are close to those of the physical environment. Our representation of the spatial distribution of capelin (predators) was probably inadequate in some respects. Although the high resolution of the hydroacoustic data permitted a more detailed picture of the spatial distribution during the course of each survey, we have no information regarding predator movement within the bay or about immigration or emigration. Migration patterns of pelagic fish can result in rapid changes in the abundance of these animals in small systems and their pattern of variation exhibits considerable variability at small time and space scales (Horne and Schneider, 1994). At the time of our study, capelin are actively migrating in and out of coastal waters (Templeman, 1948; Nakashima, 1999). Although our survey may not have captured the short-term movements of capelin with the study region, our sampling likely captured the changes in overall abundance that occurred over the study period. In a larger study site, relative movement of predators would likely be less important and a more accurate view of spatial and temporal variations in abundance could be achieved by repeated sampling. On spatial scales of 100s of kilometres and time scales of weeks, such as those studied by Heath *et al.* (1998), the extent of spatial and temporal variations in environmental features may be more readily detected in the reconstruction of environmental histories. However, we were able to provide a gross characterization of the changes in predator abundance in the inner and outer parts of the bay that allow a better interpretation of the patterns in survival.

The lack of a strong relationship with the prey environment suggests that events at the scale of the individual may be more important in determining an individual's growth and survival potential than the prey field described by large-scale surveys with station separations on the order of several kilometres. Unfortunately, processes at the individual level may be particularly difficult to identify because of our inability to adequately describe environmental variation at very small scales. The effect of small-scale turbulence on radiated shanny larvae can only be characterized in broad terms with substantial changes in environmental conditions (Dower *et al.*, 1998). Factors such as parental influence may play an important role in determining an individual's growth potential (Benoît and Pepin, 1999; Grønkjær and Schytte, 1999; Hoeie *et al.*, 1999), but these may be difficult to identify in a mixed population without knowledge of the state of the adult population. There is some indication that the level of variation in growth histories within individuals may provide some insight into the characteristics of potential survivors. The distribution of growth histories within and among larvae may yield some insight into the processes that lead to different growth rates but this will require further study. Moreover, how will external selection forces determine which patterns of growth are most conducive to survival?

Although predation is one of the major factors influencing patterns of survival in larval fish, it is also one of the most poorly understood (Bailey and Houde, 1989). Laboratory and enclosure studies have demonstrated that the vulnerability of fish larvae to predators is dependent on the size of both prey and predator (Bailey and Houde, 1989; Fuiman and Margurran, 1994; Paradis *et al.*, 1996; Sogard, 1997). Maximum vulnerability occurs when larval length is 10% of the predator length and decreases on either side of this value (Paradis *et al.*, 1996). In this study, we focussed on the predatory role of pelagic fish because previous work indicated that invertebrate carnivores, which are mostly small, were unlikely to generate mortality rates in excess of 0.001 day^{-1} in Conception Bay (Paradis and Pepin, 2001). Although we were unable to find a pattern of mortality in relation to predator abundance that was consistent with the expectation of a positive trend, both the increase in mortality with increasing length and the selective removal of fast-growing larvae from the population suggests that pelagic fish are likely to be an important factor influencing losses from the population. Capelin sampled in Conception Bay in 1998 range from 5 to 18 cm in length, which implies that as larval fish increase in length, they should become more vulnerable to this predator. Until predation pressure is reduced (e.g. through emigration out of the area), low growth rates are likely to provide a short-term survival advantage when considered over a fixed time interval (Paradis *et al.*,

1999). However, before we can move beyond deducing the role of pelagic fish in determining patterns of larval survival from corollaries we must better understand the patterns of encounter between prey and predator.

Our inference about the probable role of capelin on the dynamics of larval radiated shanny would have benefited from corroborating evidence from stomach content analysis. Capelin, like many other planktivorous marine fish, feed on a variety of prey, including fish eggs and larvae. However, as Hunter and Kimbrell (1980) point out, larval fish are poorly represented in diet analyses because of their rapid digestion time (<30 min). The time scale for digestion of larval fish is similar to the time required to launch and retrieve the trawl and process the catch for stomach analysis. Therefore, it is difficult to establish the impact that planktivores may have on larval fish from stomach analysis. However, the feeding of capelin on other prey types that are less rapidly digested may provide some insight if prey of similar size and escape ability are found in the stomachs. Vésin *et al.* (1981), Huse and Toresen (1996) and Astthorsson and Gislason (1997) found that although copepods (e.g. *Calanus finmarchicus*) are the numerically dominant prey of capelin, euphausiids (e.g. *Thyssanoessa* sp.) often make up a significant proportion of the biomass in the stomachs. These euphausiids range in size from 5 to 15 mm total length, an interval comparable to the size range of larvae considered in this study. Furthermore, short-term patch studies found good correspondence between the density of capelin and the mortality rate of radiated shanny larvae after correcting for dispersive losses (Pepin *et al.*, 2002). Thus, it is not unreasonable to conclude that the pattern of mortality for larval radiated shanny in our study is the result of predation by juvenile and adult capelin.

A few field studies dealing with the potential impact of invertebrate carnivores on larval fish have found evidence that mortality rates are correlated with the abundance of these predators and can lead to spatial differences in population dynamics (Taggart and Leggett, 1987; Rilling and Houde, 1999). The predatory influence of pelagic fish has been more difficult to quantify (Pepin *et al.*, 2002), although there is evidence of increased egg mortality with higher pelagic fish abundance (Smith *et al.*, 1989). The positive association of mortality with invertebrate carnivore levels may be more easily detected, because both prey and predator are similarly subject to advection, which could maintain spatial and temporal overlap, so that the impact can be identified. In a *post hoc* analysis, we were able to characterize two broad regions (inner and outer bay) with substantially different environmental histories in terms of predator abundance. Drift of larvae from the inner to the outer bay (i.e. from a region of apparent low predator abundance to one with higher levels), was also associated with the disappearance of fast-growing larvae from the population by the end of the second week. However, the short-term changes that took place between surveys did not provide an adequate description of the encounters between predator and prey. This is in contrast with a series of short-term patch studies that show greater population losses in the presence of greater numbers of juvenile and adult capelin (Pepin *et al.*, 2002). Intensive surveys of local conditions enabled us to follow fluctuations in environmental conditions more closely than could be done on a broader scale and thus we could identify substantial differences among systems that covered a large range in levels of predator abundance. Moving from small spatial and short temporal scales of observation to local or population levels requires better approaches to describing the movement of active predators.

ACKNOWLEDGEMENTS

We thank T. Shears for his efforts to coordinate the logistic and technical activities in both the field and in the laboratory. The assistance of H. Benoît, A. Bochdansky, S. Carter and K. Fleming in the field was invaluable and the careful analysis of otolith microstructure by C. Mercer is gratefully acknowledged. Comments from two reviewers helped to improve this manuscript. The work could not have been carried out without the assistance and expertise of the officers and crew of the *Wilfred Templeman*.

REFERENCES

Astthorsson, O.S. and Gislason, A. (1997) On the food of capelin in the subarctic waters north of Iceland. *Sarsia* **82:**81–86.

Bailey, K.M. and Houde, E.D. (1989) Predation on eggs and larvae of marine fishes and the recruitment problem. *Adv. Mar. Biol.* **25:**1–83.

Benoît, H.P. and Pepin, P. (1999) The interaction of rearing temperature and maternal influence on egg development rates and larval size at hatch in Yellowtail flounder (*Pleuronectes ferrugineus*). *Can. J. Fish. Aquat. Sci.* **56:**785–794.

Bowen, A.J., Griffin, D.A., Hazen, D.G., Matheson, S.A. and Thompson, K.R. (1995) Shipboard nowcasting of shelf circulation. *Cont. Shelf Res.* **15:**155–128.

Davidson, F.J.M. and deYoung, B. (1995) Modeling advection of cod eggs and larvae on the Newfoundland Shelf. *Fish. Oceanogr.* **4:**33–51.

Davidson, F.J.M., Greatbatch, R.J. and deYoung, B. (2001) Asymmetry in the response of a stratified coastal embayment to wind forcing. *J. Geophys. Res.* **106:**7001–7016.

Davis, T.L.O., Lyne, V. and Jenkins, G.P. (1991) Advection, dispersion and mortality of a patch of southern bluefin tuna larvae *Thunnus maccoyii* in the East Indian Ocean. *Mar. Ecol. Prog. Ser.* **73:**33–45.

deYoung, B., Otterson, T. and Greatbatch, R.J. (1993) The local and nonlocal response of Conception Bay to wind forcing. *J. Phys. Oceanogr.* **23:**2617–2635.

Dower, J.F., Pepin, P. and Leggett, W.C. (1998) Enhanced gut fullness and an apparent shift in size-selectivity by radiated shanny (*Ulvaria subbifurcata*) larvae in response to increased turbulence. *Can. J. Fish. Aquat. Sci.* **55:**128–142.

Fuiman, L.A. and Margurran, A.E. (1994) Development of predator defences in fishes. *Rev. Fish Biol.* **4:**145–183.

Gallego, A., Heath, M.R., McKenzie, E. and Cargill, L.H. (1996) Environmentally induced short-term variability in the growth rates of larval herring. *Mar. Ecol. Prog. Ser.* **137:**11–23.

Greatbatch, R.J. and Otterson, T. (1991) On the formulation of open boundary conditions at the mouth of a bay. *J. Geophys. Res.* **96:**18431–18445.

Grønkjær, P. and Schytte, M. (1999) Non-random mortality of Baltic cod larvae inferred from otolith hatch-check sizes. *Mar. Ecol. Prog. Ser.* **181:**53–59.

Heath, M., Zenitani, H., Watanabe, Y., Kimura, R. and Ishida, M. (1998) Modelling the dispersal of larval Japanese sardine, *Sardinops melanostictus*, by the Kuroshio current in 1993 and 1994. *Fish. Oceanogr.* **7:**335–346.

Hoeie, H., Folkvord, A. and Johannessen, A. (1999) Maternal, paternal and temperature effects on otolith size of young herring (*Clupea harengus* L.) larvae. *J. Exp. Mar. Biol. Ecol.* **234:**167–184.

Horne, J.K. and Schneider, D.C. (1994) Lack of spatial coherence of predators with prey: a bioenergetic explanation for Atlantic cod feeding on capelin. *J. Fish. Biol.* **45:**191–207.

Hunter, J.R. and Kimbrell, C.A. (1980) Egg cannibalism in the northern anchovy, *Engraulis mordax*. *Fish. Bull.* **78:**811–816.

Huse, G. and Toresen, R. (1996) A comparative study of the feeding habits of herring (*Clupea harengus*, Clupeidae, L.) and capelin (*Mallotus villosus*, Osmeridae, Müller) in the Barents Sea. *Sarsia* **81:**143–153.

Laprise, R. and Pepin, P. (1995) Factors influencing the spatio-temporal occurrence of fish eggs and larvae in a northern, physically-dynamic coastal environment. *Mar. Ecol. Prog. Ser.* **122:**73–92.

Litvak, M.K. and Leggett, W.C. (1992) Age and size-dependent predation on larval fishes: the bigger-is-better hypothesis revisited. *Mar. Ecol. Prog. Ser.* **81:**13–24.

MacLennan, D.N. and Simmonds, J.E. (1992) *Fisheries Acoustics*. London: Chapman and Hall, 325pp.

Mosegaard, H., Svedang, H. and Taberman, K. (1988) Uncoupling of somatic and otolith growth rates in Arctic char (*Salvelinus alpinus*) as an effect of differences in temperature response. *Can. J. Fish. Aquat. Sci.* **45:**1514–1524.

Murdoch, R.C. and Quigley, B. (1994) Patch study of mortality, growth and feeding of the southern gadoid *Macruronus novaezelandiae*. *Mar. Biol.* **121:**23–33.

Nakashima, B.S. (1999) Results of the 1998 aerial survey of capelin (*Mallotus villosus*) schools. In: *Capelin in SA2 + Div. 3KL*. Anonymous (ed.). Canadian Stock Assessment Secretariat Research Document 99/206, pp. 59–70.

Paradis, A.R. and Pepin, P. (2001) Modeling changes in the length frequency distributions of fish larvae using field estimates of predator abundance and size distributions. *Fish. Oceanogr.* **10:**217–234.

Paradis, A.R., Pepin, P. and Brown, J.A. (1996) Vulnerability to predation of fish eggs and larvae: a review of the influence of the relative size of prey and predator. *Can. J. Fish. Aquat. Sci.* **53:**1226–1235.

Paradis, A.R., Pépin, M. and Pepin, P. (1999) An individual-based model of the size-selective vulnerability of fish larvae to four major predator types: disentangling the effect of size-dependent encounter rates and susceptibility to predation. *Can. J. Fish. Aquat. Sci.* **56:**1562–1575.

Pepin, P., Evans, G.T. and Shears, T.H. (1999) Patterns of RNA/DNA ratios in larval fish and their relationship to survival in the field. *ICES J. Mar. Sci.* **56:**697–706.

Pepin, P., Dower, J.F. and Benoît, H.P. (2001) The role of measurement error on the interpretation of otoltih increment width in the study of growth in larval fish. *Can. J. Fish. Aquat. Sci.* **58:**2204–2212.

Pepin, P., Dower, J.F., Helbig, J.A. and Leggett, W.C. (2002) Regional differences in mortality rates of a larval fish, the radiated shanny (*Ulvaria subbifurcata*): estimating the relative roles of dispersal and predation. *Can. J. Fish. Aquat. Sci.* **59:**105–114.

Pepin, P. and Shears, T.H. (1997) Variability and capture efficiency of bongo and Tucker trawl samplers in the collection of ichthyoplankton and other macrozooplankton. *Can. J. Fish. Aquat. Sci.* **54:**765–773.

Rilling, G.C. and Houde, E.D. (1999) Regional and temporal variability in growth and mortality of bay anchovy, *Anchoa mitchilli*, larvae in Chesapeake Bay. *Fish. Bull.* **97:**555–569.

Rose, G.A. (1998) Acoustic target strength of capelin in Newfoundland waters. *ICES J. Mar. Sci.* **55:**918–923.

Smith, P.E., Santander, H. and Alheit, J. (1989) Comparison of the mortality rates of Pacific sardine, *Sardinops sagax*, and Peruvian anchovy, *Engraulis ringens*, eggs off Peru. *Fish. Bull.* **87:**497–508.

Sogard, S.M. (1997) Size-selective mortality in the juvenile stage of teleost fishes: a review. *Bull. Mar. Sci.* **60:**1129–1157.

Sokal, R.S. and Rohlf, F.J. (1981) Biometry, 2nd edn. New York: W. H. Freeman and Company, 859 pp.

Taggart, C.T., Thompson, K.R., Maillet, G.L., Lochman, S.E. and Griffin, D.A. (1996) Abundance distribution of larval cod (*Gadus morhua*) and zooplankton in a gyre-like water mass on the Scotian Shelf. In: *Survival Strategies in Early Life Stages of Marine Resources*. Y. Watanabe, Y. Yamashita and Y. Oozeki (eds). Rotterdam: A.A. Balkema, pp. 155–173.

Taggart, C.T. and Leggett, W.C. (1987) Short-term mortality in post emergent capelin *Mallotus villosus*. I. Analysis of multiple in situ estimates. *Mar. Ecol. Prog. Ser.* **41:**205–217.

Templeman, W. (1948) The life history of the capelin (*Mallotus villosus* O.F. Müller) in Newfoundland waters. *Res. Bull. Nfld. Gov. Lab.* **17:**1–151.

Vésin, J.P., Leggett, W.C. and Able, K.W. (1981) Feeding ecology of capelin (*Mallotus villosus*) in the estuary and western Gulf of St. Lawrence and its multispecies implications. *Can. J. Fish. Aquat. Sci.* **38:**257–267.